Composite Structures 93 (2011) 456–464

Contents lists available at ScienceDirect

Composite Structures

journal homepage: www.elsevier.com/locate/compstruct

Assessments of refined theories for buckling analysis of laminated plates

P. Nali *, E. Carrera **, S. Lecca

Department of Aeronautics and Space Engineering, Politecnico di Torino, Corso Duca Degli Abruzzi, 24-10129 Turin (TO), Italy

ARTICLE INFO

Article history:
Available online 6 September 2010

Keywords:
Buckling analysis
Advanced finite elements
Higher order plate modelling
Layer-Wise description

ABSTRACT

Linearized buckling analysis of laminated plates subjected to combined bi-axial/shear loading is described in this work. Isotropic, orthotropic and anisotropic plates are referred to. Two-dimensional plate modelling is considered. The Principle of Virtual Displacement (PVD) is applied. The Finite Element Method (FEM) is adopted in order to approximate the solution. The same cases-study are handled using different kinds of plate Finite Elements (FEs), with the purpose of providing some guidelines/benchmarks useful for identifying the most appropriate modelling for each class of buckling problem. The considered set of FEs is hierarchical in the sense that a variable kinematics approach is employed: both Equivalent Single Layer (ESL) and Layer-Wise (LW) variable descriptions are implemented, keeping the expansion order for thickness variables generic. FE matrices are obtained in compact form by referring to Carrera's Unified Formulation (CUF). When available, exact solutions are referred to in order to assess the FEM results.

1. Introduction

The buckling phenomenon consists of a sudden change of equilibrium configuration at a certain critical load. The *i*th critical load can be calculated through stability analysis, identifying the corresponding *i*th bifurcation point. The most general approach for buckling analysis requires the solving of complex nonlinear equilibrium and stability equations [1,2]. Moreover, these computationally expensive solutions should be performed together with a reliability analysis in order to account for the probabilistic nature of real perturbation sources [3]. As summarized in a previous paper [4], a simplified method to perform buckling analysis can be by interpreting the critical load as the load at which more than one infinitesimally adjacent equilibrium configuration exists (bifurcation point). If a linear initial equilibrium path is also assumed, linearized stability analysis reduces the determination of the critical load to a linear eigenvalue problem (Euler's method) [5]. This simplified approach can be conveniently applied to flat plates because the critical equilibrium configuration shows a gradual geometry change when the load passes through the critical level. An extension of the eigenvalue approach to imperfection sensitive cylindrical shells has been proposed by retaining a nonlinear pre-buckling deformation [6]. However, despite today's computing performances offering a robust nonlinear stability analysis, in shell design practice the conservative lower-bound design philosophy developed in the late 1960s and 1970s is still widely used [7,8]. In this design method, the allowable critical load predicted through the linearized analysis is reduced by an empirical knockdown factor that accounts for the degrading effects of uncertainties and imperfections linked to geometry, material as well as loading and boundary conditions. Efforts are currently directed towards the improvement of the excessively conservative and deterministic knockdown factors originally found for isotropic shells upon consideration of composite fabrication processes and probabilistic aspects [9–11].

Buckling is one of the characteristic failure modes of thin structures like plates and shells. These structures are largely employed the aerospace industry under the form of multilayered composite panels, with generic stacking sequence. The deflection of a generic panel after buckling is in general quite relevant. Contacts and interactions among the components under buckling and the rest of the structure have to be accounted for in the design process, if buckling is allowed in design-requirements. The buckling behavior is strongly affected by small perturbation of the nominal initial configuration and by structural imperfections, which can lead to a catastrophic failures at load levels far below those predicted by a simplified analysis method. A comprehensive state-of-the-art review on the buckling of composite plates was presented by Leissa [12,13].

A layered panel with generic stacking sequence/load-kind may not exhibit buckling. Some conditions regarding the staking

* Corresponding author.
** Corresponding author.
E-mail addresses: pietro.nali@polito.it (P. Nali), erasmo.carrera@polito.it (E. Carrera), saverio.lecca@polito.it (S. Lecca).
URLs: http://www.mul2.com (P. Nali), http://www.mul2.com (E. Carrera), http://www.mul2.com (S. Lecca).

0263-8223/$ - see front matter © 2010 Elsevier Ltd. All rights reserved.
doi:10.1016/j.compstruct.2010.08.035

sequence/load-kind have to be satisfied in order to have buckling. Harris [14] and Prabhakara [15] presented the post-buckling behavior of antisymmetric angle- and cross-ply plates, respectively. Harris [14] demonstrated the existence of bifurcation buckling for regular antisymmetric angle-ply plates under uniaxial or biaxial compression and stated that it does not exist for generally asymmetric angle-ply plates. Singh and Sadasiva Rao [16] and Singh et al. [17] studied the bifurcation buckling of unsymmetrically laminated rectangular plates under uniform and linearly varying edge compression, respectively, wherein the pre-buckling stress analysis is carried out by constraining the out-of-plane displacements to be zero. These transverse displacements are constrained based on the assumption that if these deformations are present during the pre-buckling regime, then bifurcation instability may not take place. Leissa [18] investigated the conditions for unsymmetrically laminated plates to remain flat during the pre-buckling stage when subjected to in-plane loads (uniaxial/or biaxial compression and/or shear). Singh *et al.* [19] studied the existence of bifurcation buckling in unsymmetrically laminated plates using an alternative approach which is more rigorous and does not involve any a priori assumptions (such as the flatness conditions of Leissa [18]). Papers [19,20] indicate that it is not necessary that the plate should remain flat during the pre-buckling regime for bifurcation buckling to occur.

The majority of aerospace structures, which can be considered an assemblage of multilayered panels supported by beams, experience a combined loading during their operational life. This implies that buckling may be caused by combined biaxial compression and shear loading. Harris, in his work [14], studied the buckling of composite plates under biaxial loading. Matsunaga [21,22] analyzed the buckling of thick elastic plates subjected to in-plane stresses, with particular emphasis on the variation of natural frequencies in preloaded condition. Ahmed et al. [23] proposed some FEM buckling solutions for multilayered composite layers subjected to in-plane and shear loadings. Ferreira et al. investigated the buckling behavior of composite shells by means of a layered formulation [24]. The same author has recently applied a meshless method in order to compute the natural frequencies of thick layered plates [25].

Since it has largely been demonstrated that appropriate kinematic description is required to properly model multilayered structures under static analysis (works [26,27] among others), it is possible that advanced modelling is also required in buckling analysis of laminated plates, especially when combined loads are simultaneously present. Unfortunately, when buckling analysis is concerned, very little attention in literature has been devoted to clarifying the dependence between accuracy in results and the kinematic description employed for plate modelling. This last point has been exhaustively clarified for static analysis: the historical review conducted in [28] has led to the following main conclusions. (1) In order to better describe the unknowns at the interface between different layers, Lekhnitskii [29] was the first to propose a so-called Zig-Zag theory, which was obtained by solving an elasticity problem involving a layered beam. (2) Two other different and independent Zig-Zag theories have been singled out. One was developed by Ambartsumian [30], who extended the well-known Reissner–Mindlin theory to layered, anisotropic plates and shells; the other approach was introduced by Reissner [31], who proposed a variational theorem that permits both displacements and transverse stress assumptions. (3) On the basis of the historical considerations detailed in paper [28], it was proposed to refer to these three theories by using the following three names: Lekhnitskii Multilayered Theory (LMT), Ambartsumian Multilayered Theory (AMT), and Reissner Multilayered Theory (RMT). As far as subsequent contributions to these three theories are concerned, it can be remarked that: (4) LMT although very promising, has almost been ignored in open literature. (5) Dozens of papers have instead been presented which consist of direct applications or particular cases of the original AMT. The contents of the original works have very often been ignored, not recognized, or not mentioned in the large number of articles published in journals written in the English language.

In recent years, a hierarchic approach with variable kinematic 2D models for composite plates and shells has been successfully developed by Carrera: the original contribution is in work [26], the summary is provided in [32] and the finite element implementation can be found in [33]. By referring to two different variational formulations as well as to Equivalent Single Layer (ESL) and Layer-Wise (LW) descriptions, hierarchically ordered approximations are introduced for the through-the-thickness behavior by means of a compact unified notation. Carrera's Unified Formulation (CUF) thus permits a systematic assessment of a large number of plate models, whose accuracy has been demonstrated to range from classic 2D models to quasi-3D descriptions for both free-vibration problems and static stress analysis [34–36].

A rigorous assessment of the 2D approximations against the buckling of composite plate/shell models was recently proposed in work [4], within the framework of the CUF and referring to analytical solutions.

In this paper, the CUF is adopted to provide accurate buckling results for laminated anisotropic plates. The classic Euler method for the prediction of bifurcation loads of composite multilayered anisotropic plates is applied. The Finite Element Method is employed in order to approximate the solution. When possible (e.g. for isotropic and orthotropic plates) assessments with analytical solutions are presented.

The aim of this work is to provide some benchmarks/guidelines for the appropriate choice of kinematic description, when isotropic/orthotropic/anisotropic multilayered plates subjected to combined biaxial and shear loading have to be modelled.

2. Considered plate theories

Thin Plate Theory (TPT), based on Cauchy, Poisson or Kirchhoff assumptions type [37–39], discards transverse shear, normal stress and through-the-thickness deformation. The displacement model related to TPT can be written in the following form:

$$\begin{aligned} u_\iota(x,y,z) &= u_{0\iota}(x,y) - z\frac{\partial u_{0z}(x,y)}{\partial \iota} \quad (\text{with}) \quad \iota = x,y \\ u_z(x,y,z) &= u_{0z}(x,y). \end{aligned} \tag{1}$$

According to this theory, the plate sections remain plane and orthogonal to the plate reference surface Ω. u_0 denotes the displacements values on Ω.

Transverse shear deformations can be introduced in the modelling according to Reissner and Mindlin's kinematic assumptions [40,41]:

$$\begin{aligned} u_\iota(x,y,z) &= u_{0\iota}(x,y) + z u_{1\iota}(x,y) \quad (\text{with}) \quad \iota = x,y \\ u_z(x,y,z) &= u_{0z}(x,y). \end{aligned} \tag{2}$$

This theory is also denoted as Shear Deformation Theory (SDT). Transverse shear stresses show *a priori* constant piece-wise distribution. In both TPT and SDT, Poisson locking phenomena is contrasted by means of the plane-stress conditions as indicated in work [42].

According to CUF, Higher Order Theories (HOTs) for displacement variables can be formulated respecting the following expansion:

$$u_\iota(x,y,z) = z^\tau u_{\tau\iota}(x,y) \quad (\text{with}) \quad \iota = x,y,z \quad (\text{and}) \quad \tau = 0,\ldots,N. \tag{3}$$

The summing convention for the repeated indexes is adopted. N is the order of expansion, which is taken as a free parameter. Higher order terms are introduced in order to refine the results obtained with TPT and SDT models. In numerical investigations, N is considered equal to three. The transverse normal strain effect is described by higher order theories.

3. Stability equations by FE

At a fixed time, the Principle of Virtual Displacements (PVD) can be written as it follows [43]:

$$\int_V \delta\boldsymbol{\epsilon}^T\boldsymbol{\sigma}dV = \delta L_e, \tag{4}$$

where V is the plate volume; δ is the variational operator; $\boldsymbol{\epsilon}$ is the strain vector; $\boldsymbol{\sigma}$ is the stress vector and L_e is the work done by external loads. By introducing standard FE discretization (Section 4.2), constitutive coefficients (Eq. (12)) and nonlinear strain-displacements relations (e.g. the von Kármán ones, in Eq. (20)), the PVD in Eq. (4) can be applied in order to obtain the governing equations in the nonlinear static undamped case [44–46]:

$$\boldsymbol{K}_s\boldsymbol{Q} = \boldsymbol{P}, \tag{5}$$

where $\boldsymbol{Q}$ is the vector of nodal primary unknowns; $\boldsymbol{K}_s$ is the structure's secant stiffness matrix that depends on $\boldsymbol{Q}$; $\boldsymbol{P}$ is the vector of nodal loads.

The static case of Eq. (5) is considered for sake of simplicity (considered nonlinearities do not affect the mass matrix):

$$\boldsymbol{K}_s\boldsymbol{Q} = \boldsymbol{P}. \tag{6}$$

Eq. (6) consists of a nonlinear system of algebraic equations, which solution would lead to various equilibrium paths of the considered structural problems.

In case of buckling analysis, the interest is focused on calculation of bifurcation points. These points are the solution of the following stability equations:

$$\begin{cases} \boldsymbol{K}_s\boldsymbol{Q} = \boldsymbol{P} \\ \boldsymbol{K}_T\boldsymbol{Q} = \boldsymbol{0}, \end{cases} \tag{7}$$

where $\boldsymbol{K}_T$ is the structure's tangent stiffness matrix associated to the equilibrium conditions. The solution of Eq. (7) leads to the bifurcation points (representative of buckling) if the two following conditions are fulfilled: two different states of equilibrium are present; the tangent matrix has zero determinant.

If the plate remains flat in case of in-plane loading (shear or axial), the relevant transverse displacements are zero. As a consequence, the equilibrium conditions in the first subsystem in Eq. (7) are fulfilled by definition. Furthermore, if the in-plane loadings increases in a proportional and uniform manner from the initial conditions (by means of λ parameter), the tangent matrix can be approximated as it follows:

$$\boldsymbol{K}_T = \boldsymbol{K} + \boldsymbol{K}_\sigma, \tag{8}$$

where $\boldsymbol{K}$ is the structure's linear stiffness matrix and $\boldsymbol{K}_\sigma$ is the initial stress matrix, which can also be written in the following form:

$$\boldsymbol{K}_\sigma = \lambda\overline{\boldsymbol{K}}_\sigma. \tag{9}$$

Finally, the eigenvalue problem can be formulated:

$$(\boldsymbol{K} + \lambda_i\boldsymbol{K}_\sigma)\boldsymbol{a}_i = \boldsymbol{0}, \tag{10}$$

where the eigenvalue λ_i is the ith buckling factor and $\mathbf{a}_i$ is the corresponding eigenvector.

4. Explict form of K and K_σ for the considered plate theories

4.1. Preliminary

Plates are two-dimensional structures in which a dimension, normally the thickness z, is negligible with respect to the others. Material and laminate reference systems are illustrated in Fig. 1.

The generic constitutive equation may be expressed through the Hooke's law:

$$\boldsymbol{\sigma} = \boldsymbol{H}\boldsymbol{\epsilon}. \tag{11}$$

The Hooke's matrix $\boldsymbol{H}$ can be written as in the following:

$$\boldsymbol{H} = \begin{pmatrix} C_{11} & C_{12} & 0 & C_{13} & 0 & 0 \\ C_{12} & C_{22} & 0 & C_{23} & 0 & 0 \\ 0 & 0 & C_{66} & 0 & 0 & 0 \\ C_{13} & C_{23} & 0 & C_{33} & 0 & 0 \\ 0 & 0 & 0 & 0 & C_{55} & 0 \\ 0 & 0 & 0 & 0 & 0 & C_{44} \end{pmatrix}. \tag{12}$$

In the particular case of isotropic homogeneous plate coefficients are determined as:

$$\begin{aligned} &C_{11} = C_{22} = C_{33} = \lambda + 2\mu; \\ &C_{12} = C_{13} = C_{23} = \lambda; \\ &C_{44} = C_{55} = C_{66} = \mu, \end{aligned} \tag{13}$$

where

$$\mu = G = \frac{E}{2(1+\nu)}, \quad \lambda = \frac{\nu E}{(1+\nu)(1-2\nu)} \tag{14}$$

are the Lamé coefficients, E is the Young modulus, G is the transverse shear modulus and ν is the Poisson ratio. Stresses and strains can be so grouped in the two respective vectors:

$$\boldsymbol{\sigma}^T = \{\sigma_{xx}\ \sigma_{yy}\ \sigma_{xy}\ \sigma_{zz}\ \sigma_{xz}\ \sigma_{yz}\}, \tag{15}$$

$$\boldsymbol{\epsilon}^T = \{\epsilon_{xx}\ \epsilon_{yy}\ \gamma_{xy}\ \epsilon_{zz}\ \gamma_{xz}\ \gamma_{yz}\}. \tag{16}$$

Strains $\boldsymbol{\epsilon}$ are related to the displacement primary unknowns

$$\boldsymbol{u}^T = \{u_x\ u_y\ u_z\}, \tag{17}$$

according to the geometrical relations

$$\boldsymbol{\epsilon} = \boldsymbol{D}\boldsymbol{u}, \tag{18}$$

where $\boldsymbol{D}$ denotes the differential operator.

If the linear case is considered:

$$\boldsymbol{D} = \begin{pmatrix} \partial_x & 0 & 0 \\ 0 & \partial_y & 0 \\ \partial_y & \partial_x & 0 \\ 0 & 0 & \partial_z \\ \partial_z & 0 & \partial_x \\ 0 & \partial_z & \partial_y \end{pmatrix}. \tag{19}$$

In case of von Kármán nonlinearities, $\boldsymbol{D}$ is inclusive of corresponding nonlinear contributions:

$$\boldsymbol{D} = \begin{pmatrix} \partial_x & 0 & \partial_x^2/2 \\ 0 & \partial_y & \partial_y^2/2 \\ \partial_y & \partial_x & \partial_x\partial_y \\ 0 & 0 & \partial_z \\ \partial_z & 0 & \partial_x \\ 0 & \partial_z & \partial_y \end{pmatrix}. \tag{20}$$

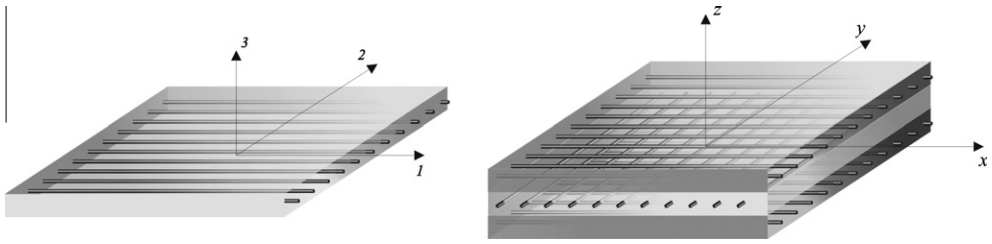

Fig. 1. Material reference system (on the left) and laminate reference system (on the right).

4.2. FEM discretization

In case of FEM implementation, the kinematic unknowns collected in vector $\mathbf{u}_\tau(x,y)$ can be expressed in terms of FE nodal values, via the shape functions N_i:

$$\boldsymbol{u}_\tau(x,y) = \sum_i N_i(x,y)\boldsymbol{Q}_{\tau i}, \quad i = 1,2,\ldots,N_n; \tag{21}$$

for virtual variations:

$$\delta\boldsymbol{u}_s(x,y) = \sum_j, N_j(x,y)\delta\boldsymbol{Q}_{sj}, \quad j = 1,2,\ldots,N_n, \tag{22}$$

where N_n denotes the number of nodes of the considered finite element. The primary unknowns are given by the expansion indices τ and i:

$$\boldsymbol{u}(x,y,z) = \sum_\tau \left\{ z^\tau \sum_i N_i \boldsymbol{Q}_{\tau i} \right\}. \tag{23}$$

4.3. Matrices $\boldsymbol{K}$

Substituting constitutive and linear geometrical relations in the variational statement of Eq. (4), focusing on the FE domain and calculating respective integrals, leads to a set of equilibrium equations which can be formally put in the following compact form:

$$\delta\boldsymbol{Q}_{sj} : \boldsymbol{K}^{k\tau sij}\boldsymbol{Q}_{\tau i} = \boldsymbol{0}, \tag{24}$$

where superscript k is introduced in order to distinguish between quantities related to different layers. The number of obtained equations coincides with the number of introduced variables: τ and s vary from 0 to N, i and j vary from 1 to N_n. Matrix $\boldsymbol{K}^{k\tau s\ i\ j}$ is the stiffness fundamental nucleus and it consists on a 3×3 array [47]. Matrix $\mathbf{K}$ can be obtained by expanding the superscript indices of $\boldsymbol{K}^{k\tau sij}$ and by running the standard assembly procedure. Here is the explicit form of the fundamental nucleus:

$$\boldsymbol{K}^{k\tau sij} = \int_{V_{el}} F_s N_j \boldsymbol{D}^T \boldsymbol{H}^k \boldsymbol{D} N_i F_\tau dV_{el}, \tag{25}$$

where V_{el} is the element volume and $\boldsymbol{D}$ is the linear differential operator in Eq. (19). If integrals are calculated via Gauss numerical integration, the corresponding plate FE could be affected by the shear locking phenomenon. In order to overcome the shear locking problem, the shear-selective Gauss integration can be adopted for shape functions [48]. A more efficient method to avoid the shear locking phenomenon consists on the Mixed Interpolation of Tensorial Components (MITC) technique. Additional details on this topic can be found in work [48], together with the explicit form of the MITC stiffness fundamental nucleus. Numerical results presented in this paper are obtained with the MITC plate FE with four nodes: MITC4.

4.4. Matrix $\boldsymbol{K}_\sigma$

Since plates are considered, only the third diagonal component of $\boldsymbol{K}_\sigma^{k\tau sij}$, is different from zero:

$$\begin{aligned}\boldsymbol{K}_\sigma^{k\tau sij}(3,3) = \sigma^0_{xx} \lessdot z^\tau z^s \gtrdot_{z_e^k} \lhd N_{i,x} N_{j,x} \rhd_{\Omega_e} + \sigma^0_{yy} \lessdot z^\tau z^s \gtrdot_{z_e^k} \\ \lhd N_{i,y} N_{j,y} \rhd_{\Omega_e} + \sigma^0_{xy} \lessdot z^\tau z^s \gtrdot_{z_e^k} \lhd N_{i,x} N_{j,y} \rhd_{\Omega_e}.\end{aligned} \tag{26}$$

Subscripts after a comma indicate derivatives, while

$$\lhd \cdots \rhd_{\Omega_e} = \int_{\Omega_{el}} (\cdots) d\Omega_{el} \qquad \text{and} \qquad \lessdot \cdots \gtrdot_{z_e^k} = \int_{k^{th\ layer}} (\cdots) dz_{k^{thlayer}}.$$

Through Eq. (26) the in-plane excitations σ^0_{xx}, σ^0_{yy}, σ^0_{xy} can be directly assigned in the model. They can appear singularly or in various combinations.

The initial stress matrix $\boldsymbol{K}_\sigma$ can be obtained from $\boldsymbol{K}_\sigma^{k\tau s\ ij}$ expanding the superscripts.

The ith buckling load is given by the previously assigned excitations σ_{xx}, σ_{yy}, σ_{xy}, multiplied by the ith eigenvalue of Eq. (10), which is indicated as buckling factor. Multiplicating σ_{xx}, σ_{yy}, σ_{xy} by the thickness of the plate leads to the in-plane force for unit length N_{xx}, N_{yy}, and N_{xy}.

5. Numerical results and discussion

Several assessments are given in this section in order to verify the effectiveness of the proposed hierarchical kinematic models. When possible, reference to available exact solutions is made. Convergence properties are illustrated for both isotropic and anisotropic multilayered plate FEs. The accuracy of TPT, SDT and HOT kinematic descriptions is illustrated for isotropic panels. Layer-Wise modelling with second order expansion for thickness variables (acronym LD2) is employed in order to provide accurate results for multilayered plates. Particular attention is devoted to the choice of the stacking sequence/fiber orientation. The effects of boundary conditions are also described. The analysis of isotropic plates has been performed considering a panel with the following properties (if not differently specified). Dimensions: $a = b$ and $h = 0.001$ m; Young Modulus: $E = 73$ GPa; Poisson's ratio: $\nu = 0.3$.

Concerning multilayered plates: $a = b$, $h = 0.001$ m (total thickness is fixed independently on the number of layers); laminae Elastic Modules: $E_1/E_2 = 30$, $G_{12}/E_2 = G_{13}/E_2 = 0.5$, $G_{23}/E_2 = 0.2$; laminae Poisson's ratio $\nu = 0.3$. Different load cases are considered and they are indicated with the following acronyms:

UAC (Uni-Axial Compression);
BAC (Bi-AxialCompression);
PS (Pure Shear);
UAS (Uni-Axialcompression and Shear);
BAS (Bi-Axial compression and Shear).

Boundary conditions at the four plate edges are denoted by a series of four letters indicating the constraint applied to the corresponding plate edges: **S**, **C** and **F** denote, simply supported,

clamped and free edge, respectively. The first letter refers to the side defined by $y = 0$ and the others follow in an anticlockwise sense.

5.1. Preliminary assessments

A four edge simply supported isotropic plate is considered in Table 1. Non-dimensional buckling loads, calculated with different kinematic models or FE meshes, are listed for different choices of thickness ratio a/h. Table 2 shows the difference between ESL and LW FEM results for a thin and a thick [0/90/0] plate with respect to the analytical solutions available in [4]; three letter acronyms are introduced to identify some additional type of kinematic assumption considered for the implemented FEs. The first letter is "E" or "L" in the case of ESL or LW variable descriptions,

Table 1
Buckling load of isotropic **SSSS** plate under **UAC**: $N_y \frac{b^2}{\pi^2 D}$. Analytical solutions and FEM results (with mesh details).

	$a/h = 10$	$a/h = 100$
TPT	4.000	4.000
[50]	3.729	3.997
[51]	3.787	3.998
[52]	3.730	3.997
[53]	3.771	3.998
SDT 10×10	3.871	4.054
SDT 20×20	3.833	4.012
HOT 10×10	3.850	4.057
HOT 20×20	3.810	4.013

Table 2
Buckling load of [0/90/0] **SSSS** plate under **UAC**: $N_y \frac{b^2}{E_2 h^2}$; mesh: 10×10.

	$a/h = 10$		$a/h = 100$	
	FEM	[4]	FEM	[4]
TPT	20.0346	19.7124	20.0347	19.7124
SDT	15.7988	15.3513	19.9801	19.6551
ED1	15.7988	16.1310	19.9801	19.9475
ED2	15.7939	–	19.9761	–
ED3	15.0918	–	19.9636	–
ED4	15.0912	15.3440	19.9636	19.6551
LD1	15.3908	15.5145	20.0004	19.7017
LD2	15.0868	–	19.9635	–
LD3	15.0771	–	19.9634	–
LD4	15.0771	15.3127	19.9634	19.6547

Table 3
Buckling load of [0/90/0] **SSSS** plate under **UAC**: $N_y \frac{b^2}{E_2 h^2}$; mesh: 10×10.

	$E_1/E_2 = 3$		$E_1/E_2 = 10$		$E_1/E_2 = 20$	
	FEM	[4]	FEM	[4]	FEM	[4]
TPT	5.8439	5.7538	11.6770	11.4918	20.0346	19.7124
SDT	5.5333	5.3991	10.2493	9.9653	15.7988	15.3513
ED1	5.5333	–	10.2493	–	15.7988	–
ED2	5.5239	5.3556	10.2449	9.9945	15.7939	15.6458
ED3	5.4745	5.3060	9.9803	9.7720	15.0918	15.0551
ED4	5.4744	–	9.9800	–	15.0912	–
LD1	5.5294	–	10.1116	–	15.3908	–
LD2	5.4736	5.3066	9.9783	9.7710	15.0868	15.0523
LD3	5.4729	–	9.9751	–	15.0771	–
LD4	5.4729	–	9.9751	–	15.0771	–
	$E_1/E_2 = 30$		$E_1/E_2 = 40$			
	FEM	[4]	FEM	[4]		
TPT	28.3950	27.9357	36.7561	36.1597		
SDT	20.3065	19.7566	24.0515	24.4529		
ED1	20.3065	–	24.0515	–		
ED2	20.3012	20.4027	24.0460	24.4816		
ED3	19.1100	19.3785	22.3695	23.0021		
ED4	19.1090	–	22.3681	–		
LD1	19.5944	–	23.0346	–		
LD2	19.1013	19.3584	22.3567	22.9690		
LD3	19.0823	–	22.3262	–		
LD4	19.0823	–	22.3262	–		

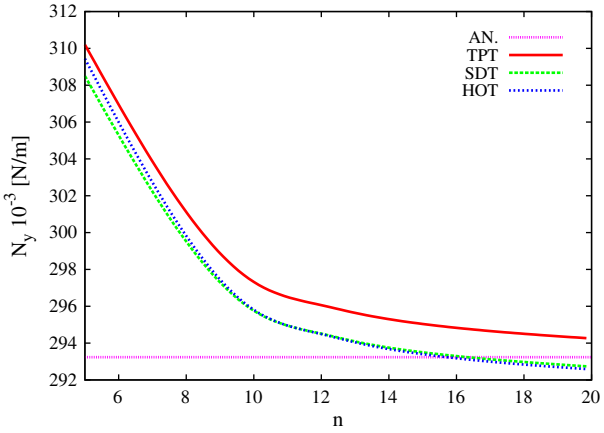

Fig. 2. Buckling loading – isotropic plate under **UAC**. Mesh $n \times n$, $a/h = 30$, $a = b$, **SSSS**.

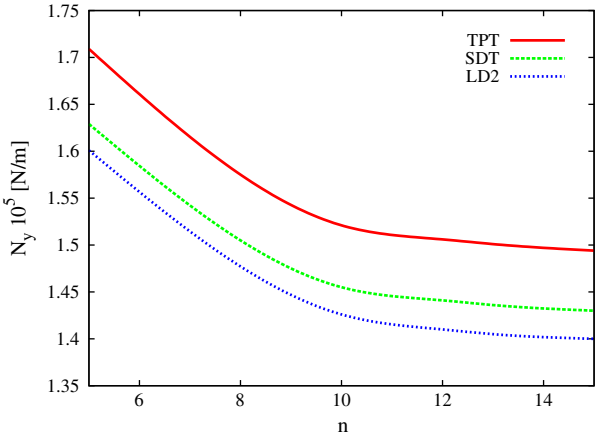

Fig. 3. Buckling loading – [0/90/0] plate under **UAC**. Mesh $n \times n$, $E_1/E_2 = 30$ a/h=30, $a = b$, **SSSS**.

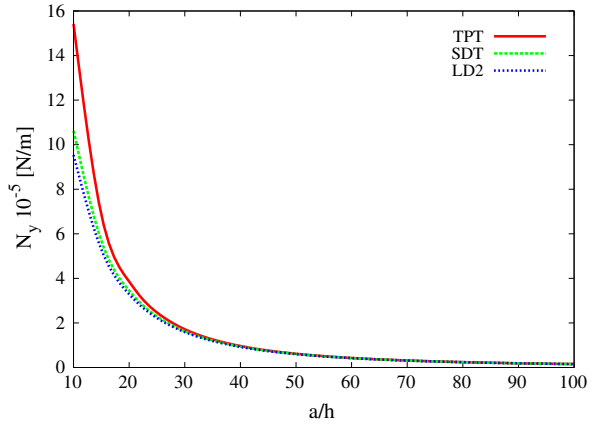

Fig. 4. Buckling loading – [0/90/0] plate under **UAC**. Mesh 10×10, $E_1/E_2 = 30$, $a = b$, **SSSS**.

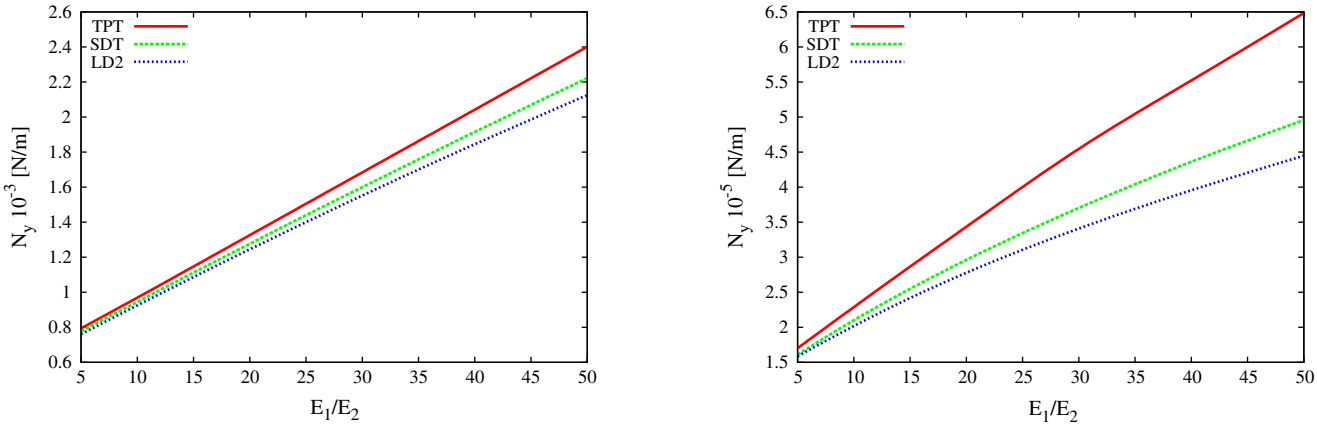

Fig. 5. Buckling loading – [0/90/0] plate under **UAC**. Mesh 15 × 15, $a/h = 30$, $a = b$, **SSSS** (left) and **CCCC** (right).

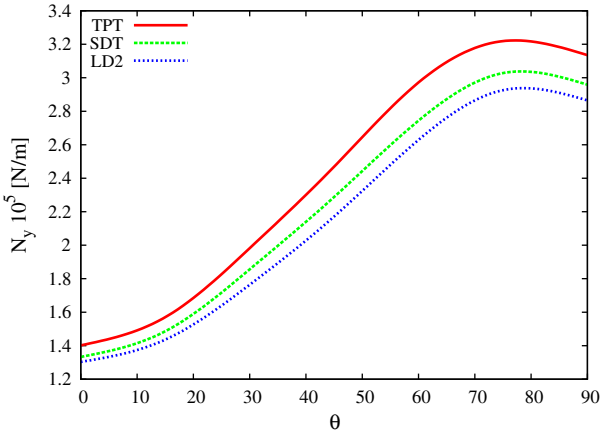

Fig. 6. Buckling loading – [0/θ/90/θ/0] plate under **UAC**. Mesh 10 × 10, $a/h = 30$, $a = b$, $E_1/E_2 = 30$, **SSSS**.

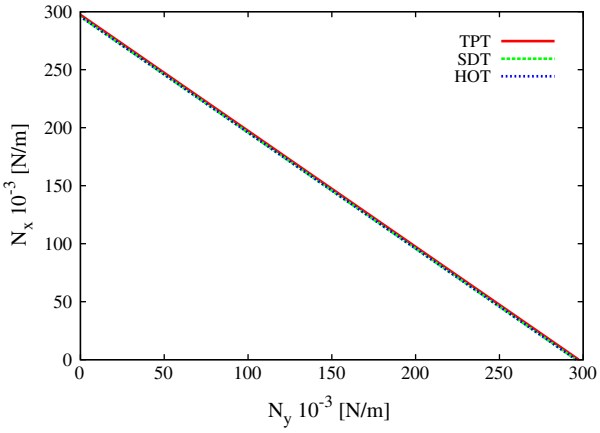

Fig. 7. Buckling loading – isotropic plate under **BAC**. Mesh 10 × 10, $a/h = 30$, $a = b$, **SSSS**.

Table 4
Buckling loads: $N_y \times 10^{-3}$ in case of **UAC**; $N_{xy} \times 10^{-3}$ in the **PS** case; $a/h = 30$; mesh: 10 × 10.

		[0/90/0]		[0/75/90/75/0]		$[45/-45]_s$	
	UAC	PS	UAC	PS	UAC	PS	
SSSS	TPT	1.714	6.706	3.219	9.250	4.295	20.306
	SDT	1.628	5.669	3.028	7.719	4.001	14.379
	LD2	1.589	5.223	2.926	7.071	3.790	12.256
CCCC	TPT	4.840	12.968	8.381	18.611	8.507	29.115
	SDT	3.912	8.838	6.738	12.365	6.836	17.066
	LD2	3.611	7.722	6.218	10.682	6.263	14.023
CSCS	TPT	3.801	12.306	5.870	16.966	6.713	25.309
	SDT	3.179	8.261	4.759	11.645	5.425	15.969
	LD2	2.984	7.117	4.382	10.007	4.968	13.285

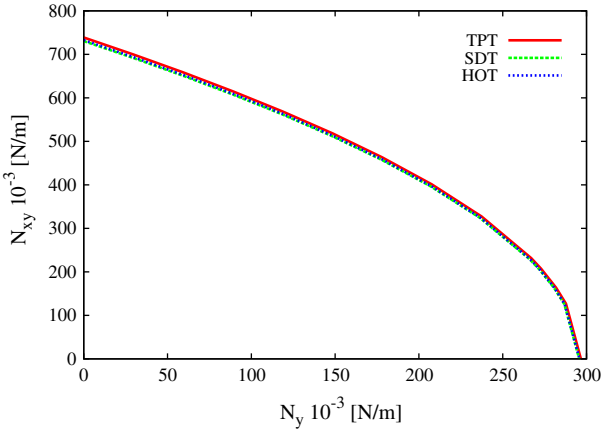

Fig. 8. Buckling loading – isotropic plate under **UAS**. Mesh 10 × 10, $a/h = 30$, $a = b$, **SSSS**.

respectively. The second letter is "D" since the PVD is applied. The number identifies the order of the through-the-thickness expansion. Within this framework, LD2 means that LW PVD FE with second order thickness expansion is considered. An additional assessment with the analytical solutions of work [4] is provided in Table 3, where the anisotropy ratio E_1/E_2 is the free parameter. The influence of the mesh refinement on the isotropic plate results is clarified in Fig. 2: the kinematic assumptions imply a slight influence on the computed buckling loads. The reference solution can be found in work [49] and is obtained with TPT assumptions. Fig. 3 shows that the LW modelling is required in order to obtain accurate results in the case of cross-ply plates. In fact, in this case the difference among TPT and SDT theories compared to LD2 is significant. No relevant differences arise if the plate is very thin, as illustrated in Fig. 4. Moreover, from Fig. 5 it can be concluded that TPT and SDT models are not appropriate when the anisotropy ratio is significant, independent of boundary conditions. This would

Table 5
Buckling load $N_x \times 10^{-5}$ of [0/90/0] **SSSS** plate under **UAC**; $a/h = 30$; mesh 10×10.

	$m = 1, n = 1$	$m = 2, n = 1$	$m = 3, n = 1$
TPT	1.895	5.050	6.615
SDT	1.829	4.880	5.713
ED2	1.828	4.884	5.712
ED3	1.799	4.835	5.369
ED4	1.799	4.835	5.369
LD1	1.796	4.858	5.280
LD2	1.786	4.814	5.220
LD3	1.786	4.811	5.219
LD4	1.786	4.811	5.219

encourage the use of higher order LW kinematic assumption in these cases (e.g. LD2 modelling).

Fig. 6 clarifies that in the case of anisotropic plates (i.e. generic fiber orientation), the errors due to the choice of the plate theory can be slightly different for certain combinations of angles through the staking sequence: in Table 4 there are some additional comparisons regarding this topic, with different stacking sequence, load cases and boundary conditions.

5.2. Isotropic homogeneous plates

The comparisons in Figs. 7 and 8 show that the accuracy of results obtained with TPT, SDT and HOT theories is almost the same in the case of isotropic plates. That is, the TPT modelling is appropriate in this case and the use of more refined kinematic descriptions is not necessary. It is interesting to note that in the case of **BAC** (Fig. 7) the curve defining the buckling loading is a straight line. Moreover, the point on the x-axis (y-axis) is representative of **UAC** along the x-axis (y-axis). Concerning **UAS** (Fig. 8), the buckling combined load is described by a non-straight line which recalls a parabolic trend.

5.3. Multilayered orthotropic and anisotropic plates

5.3.1. Uniaxial and pure shear loadings

In Table 5, some buckling loads are listed for a [0/90/0] plate with the **UAC** load case. In order to describe the buckling modes, m and n in Table 5 indicate the number of half-waves along the x- and y-directions, respectively. Results obtained with different models are compared and it can be noted that TPT theory is the least accurate since it totally neglects the contribution of shear. In this case, the ED3 and LD2 models seem the most convenient since they provide results very close to those obtained with LD4 theory and, at the same time, they involve a smaller number of degrees of freedom.

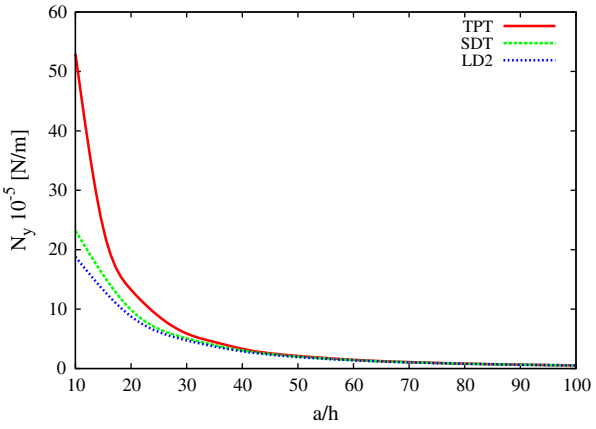

Fig. 10. Buckling loading – [0/90/0] plate under **PS**, Mesh 10×10, $E_1/E_2 = 25$, $a = b$, **SSSS**.

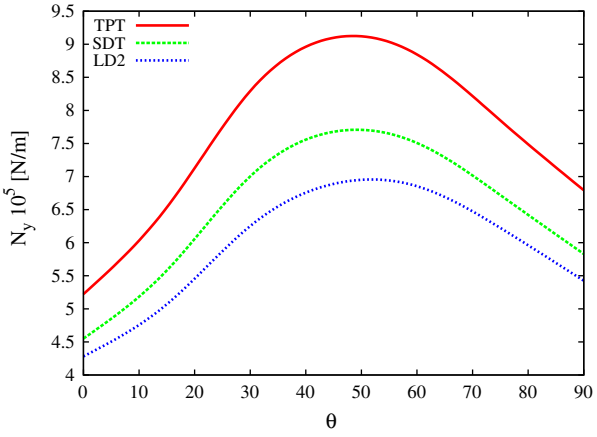

Fig. 11. Buckling loading – [0/θ/90/θ/0] plate under **PS**. Mesh 10×10, $E_1/E_2 = 25$, $a/h = 30$, $a = b$, **SSSS**.

The effect of pure shear loading is described in Figs. 9–11. Figs. 9 and 10 illustrate that a refined modelling technique is required in order to analyze plates with high orthotropic or high thickness ratios, respectively. According to Fig. 9, an advanced kinematic description is in general required when dealing with orthotropic materials: the error is perceivable also with $E_1/E_2 = 5$. Moreover, there is no substantial difference between square and non-square

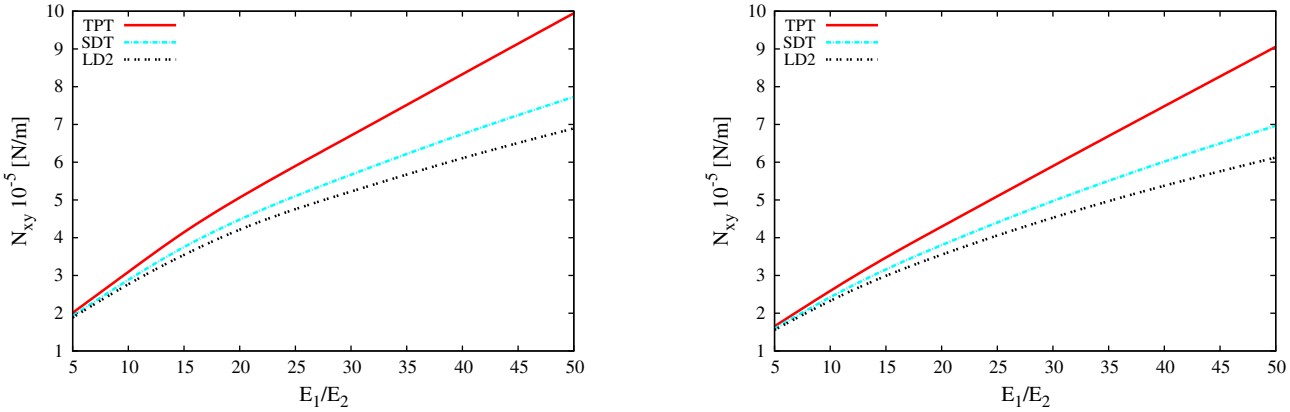

Fig. 9. Buckling loading – [0/90/0] plate under **PS**, $a/h = 30$, **SSSS**. Left: Mesh 10×10, $a = b$. Right: Mesh 8×24, $a = 3b$.

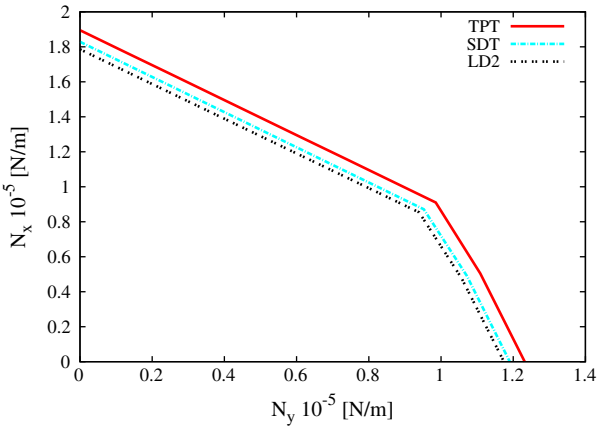

Fig. 12. Buckling loading – [0/90/0] plate under **BAC**, Mesh 10 × 10, E_1/E_2 = 16.7, a/h = 30, a = b, **SSSS**.

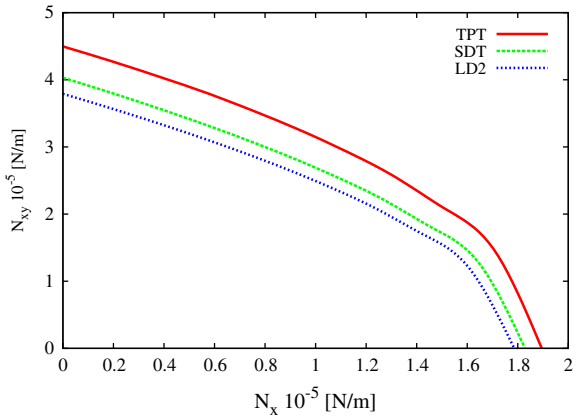

Fig. 13. Buckling loading – [0/90/0] plate under **UAS**, Mesh 10 × 10, E_1/E_2 = 16.7, a/h = 30, a = b, **SSSS**.

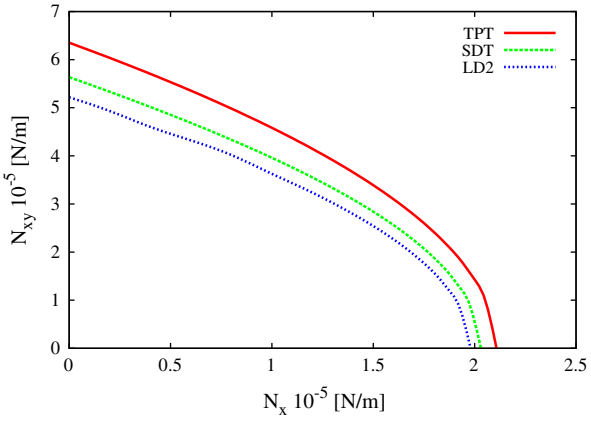

Fig. 14. Buckling loading – [0/45/90/45/0] plate under **UAS**, Mesh 10 × 10, E_1/E_2 = 16.7, a/h = 30, a = b, **SSSS**.

plates (by comparing the left and right sub-figures of Fig. 9). Concerning Fig. 10, small differences between different theories arise when $a/h < 45$. Fig. 11 shows that TPT and SDT results are different from LD2 ones and this is valid for a generic choice of fiber orientation throughout the staking sequence.

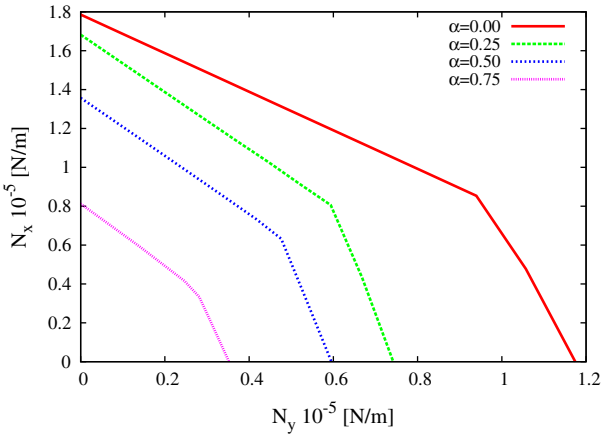

Fig. 15. Buckling loading – [0/90/0] plate under **BAS**, Mesh 10 × 10, E_1/E_2 = 16.7, a/h = 30, a = b, **SSSS**.

5.3.2. Combined loadings

The response to **BAC** load case is presented in Fig. 12. The curve slope change is due to eigenvalue crossing and then to the change in buckling mode (from 1 × 1 to 2 × 1 half-waves). It needs to be underlined that, in Fig. 12, TPT and SDT theories cannot reach the accuracy of LD2 modelling. This is due to the fact that a multilayered orthotropic panel is analyzed. In fact, in Fig. 7, which regards an isotropic plate with the same thickness ratio, there is no difference between different kinematic descriptions.

In the case of **UAS** loading, the curves become non-straight: Figs. 13 and 14 show the behavior of a cross-ply and an anisotropic plate, respectively. The effect due to the orthotropic laminae is revealed by the difference between TPT, SDT and LD2 curves. This effect is not present in Fig. 8, where the material is isotropic and there is no substantial difference between the different theories.

An example of **BAS** loading is reported in Fig. 15. Each curve corresponds to a given percentage of critical pure shear load. As one can expect, the higher the shear loading, the lower the bi-axial compression when buckling occurs.

6. Conclusions

This paper provides a set of results concerning the buckling analysis of isotropic, orthotropic and anisotropic plates. In order to make some numerical assessments, the same results have been obtained using different FEs. The considered set of FEs is hierarchical in the sense that the CUF variable kinematics approach has been employed in order to obtain the FE matrices. Different types of geometry, boundary conditions and load combinations have been considered in order to achieve some rather general conclusions. It has been deduced that, concerning isotropic plates, classical methods available in commercial software (TPT and SDT) provide results in excellent agreement with refined solutions and this has been confirmed for a wide range of geometry parameters and different load cases and boundary conditions. On the contrary, TPT and SDT theories have proved inadequate to model thick plates or multilayered plates composed of laminae with high orthotropic ratio. Accurate results for the latter problems and for the generic analysis of anisotropic plates have been provided by LW theories with higher order thickness expansion (e.g. LD2 which is not yet available in commercial software).

Future investigations could be devoted to the analysis of plates with a higher number of layers and to make comparisons with experimental results.

Acknowledgement

This work has been partially carried out in the framework of MICROCOST Project.

References

[1] Stein E. In: Stein E, de Borst R, Hughes TJR, editors. Buckling. Encyclopedia of computational mechanics, vol. 2. John Wiley & Sons; 2004.
[2] Bushnell D. Computerized buckling analysis of shells. Dordrecht: M. Nihhoff; 1985.
[3] Elishakoff I, van Manen S, Vermeulen PG, Arbocz J. First-order second-moment analysis of the buckling of shells with random imperfections. AIAA J 1987;25:1113–7.
[4] D'Ottavio M, Carrera E. Variable-kinematics approach for linearized buckling analysis of laminated plates and shells. AIAA J 2010;48:1987–97.
[5] Timoshenko SP, Gere JM. Theory of elastic stability. New York: McGraw-Hill; 1961.
[6] Jabareen M. Rigorous buckling of laminated cylindrical shells. Thin-Walled Struct 2009;47:233–40.
[7] Buckling of thin-walled circular cylinders. NASA Space Vehicle Design Criteria NASA SP-8007. NASA; 1968.
[8] ECSS Draft Standard on Buckling. P.O. Box 299, 2200 AG Noordwijk, The Netherlands: ESA Requirements and Standards Division, ESTEC; 2008.
[9] Arbocz J, Starnes Jr JH. Future directions and challenges in shell stability analysis. Thin-Walled Struct 2002;40:729–54.
[10] Hilburger MW, Starnes Jr JH. Effect of imperfections on the buckling response of compression-loaded composite shells. Int J Non-Lin Mech 2002;37:623–43.
[11] Arbocz J, Hilburger MW. Toward a probabilistic preliminary design criterion for buckling critical composite shells. AIAA J 2005;43:1823–7.
[12] Leissa AW. Buckling of laminated composite plates and shell panels. Flight Dynamics Laboratory Report No. AFWAL-TR-85-3069; 1985.
[13] Leissa AW. A review of laminated composite plate buckling. Appl Mech Rev 1987;40(5):555–79.
[14] Harris GZ. The buckling and post buckling behaviour of composite plates under biaxial loading. Int J Mech Sci 1975;17(3):187–202.
[15] Prabhakara MK. Post-buckling behaviour of simply-supported cross-ply rectangular plates. Aeronaut Quart 1976;27(4):309–16.
[16] Singh G, Sadasiva Rao YVK. Stability of thick angle-ply composite plates. Comput Struct 1988;29:317–22.
[17] Singh G, Sadasiva Rao YVK, Iyengar NGR. Buckling of thick layered composite plates under inplane moment loading. Compos Struct 1989;13(1):35–48.
[18] Leissa AW. Conditions for laminated plates to remain flat under in-plane loading. Compos Struct 1986;6(4):271–81.
[19] Singh G, Venkateswara Rao G, Iyengar NGR. Bifurcation buckling in unsymmetrically laminated plates. Compos Eng 1994;4(2):181–94.
[20] Singh G, Venkateswara Rao G, Iyengar NGR. Thermal post buckling behaviour of rectangular antisymmetric cross-ply composite plates. Acta Mech 1993;98: 39–50.
[21] Matsunaga H. Buckling instabilities of thick elastic plates subjected to in-plane stresses. Comput Struct 1995;62(1):205–14.
[22] Matsunaga H. Vibration and stability of cross-ply laminated composite plates according to a global higher-order plate theory. Comput Struct 2000;48: 231–44.
[23] Ahmed Noor K, Jeanne Peters M. Finite element buckling and postbuckling solutions for multilayered composite panels. Finite Elem Anal Des 1994;15: 343–67.
[24] Ferreira AJM, Barbosa JT. Buckling behaviour of composite shells. Compos Struct 2000;50(1):93–8.
[25] Ferreira AJM, Fasshauer GE, Batra RC. Natural frequencies of thick plates made of orthotropic, monoclinic, and hexagonal materials by a meshless method. J Sound Vib 2009;319(3-5):984–92.
[26] Carrera E. A class of two dimensional theories for multilayered plates analysis, Atti Accademia delle Scienze di Torino. Mem Sci Fis 1995;19–20:49–87.
[27] Ferreira AJM. Polyharmonic (thin-plate) splines in the analysis of composite plates. Int J Mech Sci 2004;46:1549–69.
[28] Carrera E. Historical review of zig-zag theories for multilayered plates and shells. Appl Mech Rev 2003;56:287–308.
[29] Lekhnitskii SG. Strength calculation of composite beams. Vestnik inzhen i tekhnikov 1935;9.
[30] Ambartusumian SA. On a theory of bending of anisotropic plate. Investiia Akad Nauk SSSR Ot Tekh Nauk 1958;4.
[31] Reissner E. On a certain mixed variational theory and a proposed application. Int J Numer Methods Eng 1984;20:1366–8.
[32] Carrera E. Theories and finite elements for multilayered plates and shells: a unified compact formulation with numerical assessment and benchmarking. Arch Comput Methods Eng 2003;10(3):215–96.
[33] Carrera LDeMasiE. Classical and advanced multilayered plate elements based upon PVD and RMVT. Part 1. Derivation of finite element matrice. Int J Numer Methods Eng 2002;55:191–231.
[34] Carrera E. Single layer vs multilayer plate modellings on the base of reissner's mixed theorem. AIAA J 2000;38(2):342–52.
[35] Carrera E. An assessment of mixed and classical theories on global and local response of multilayered orthotropic plates. Compos Struct 2000;50:183–98.
[36] Carrera E, Giunta G. Hierarchical evaluation of failure parameters in composite plates. AIAA J 2009;47:692–702.
[37] Cauchy AL. Sur lequilibre et le mouvement dune plaque solide. Exercises de Matematique 1828;3:328–55.
[38] Poisson SD. Memoire sur lequilibre et le mouvement des corps elastique. Mem Acad Sci 1829;8:353–570.
[39] Kirchhoff G. Uber das gleichgewicht und die bewegung einer elastishen scheibe. J Angew Math 1850;40:51–88.
[40] Reissner E. The effect of transverse shear deformation on the bending of elastic plates. J Appl Mech 1945;12:69–76.
[41] Mindlin RD. Influence of rotatory inertia and shear in flexural motions of isotropic elastic plates. J Appl Mech 1951;18:1031–6.
[42] Carrera E, Brischetto S. Analysis of thickness locking in classical, refined and mixed multilayered plate theories. Compos Struct 2008;82:549–62.
[43] Carrera E, Brischetto S, Nali P. Variational statements and computational models for multifield problems and multilayered structures. MAMS 2008;15(3):182–98 [special issue].
[44] Crisfield MA. Non-linear finite element analysis of solids and structures. The Atrium, Southern Gate, Chichester, West Sussex, England: Wiley & Sons Ltd.; 1991.
[45] Bathe KJ. Finite element procedures. Upper Saddle River (NJ): Prentice-Hall, Inc.; 1996.
[46] Zienkiewicz OC, Taylor RL, Zhu JZ. The finite element method: Its basis and fundamentals. 6th ed. Jordan Hill, Oxford: Elsevier Butterworth-Heinemann Linacre House; 2005.
[47] Carrera E. Theories and finite elements for multilayered plates and shells: a unified compact formulation with numerical assessment and benchmarking. Arch Comput Methods Eng 2003;10:215–97.
[48] Carrera E, Cinefra M, Nali P. MITC technique extended to variable kinematic multilayered plate elements. Compos Struct 2010;92:1888–95.
[49] Leissa AW. Vibration of plates. NASA SP-160; 1969.
[50] Brunelle EJ, Robertson SR. Vibrations of an initially stressed thick plate. J Sound Vib 1976;45:405–16.
[51] Reddy JN, Phan PH. Stability and vibration of isotropic, orthotropic and laminated plates according to a higher order shear deformation theory. J Sound Vib 1985;98:157–70.
[52] Doong JL. Vibration and stability of an initially stressed thick plate according to a high-order deformation theory. J Sound Vib 1987;113(3, 22):425–40.
[53] Matsunaga H. Free vibration and stability of thick elastic plates subjected to in-plane forces. Int J Solids Struct 1994;31(22):3113–24.